Technical Annals

Vol 1, No 6 (2024)

Technical Annals

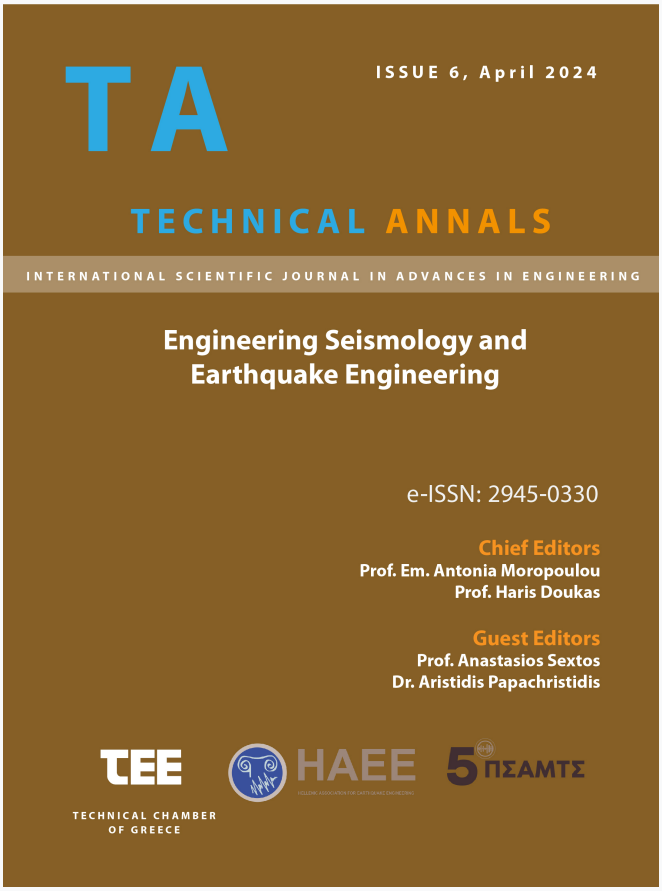

Risk Assessment of Ancient Colonnades

Spyridon Diamantopoulos, Michalis Fragiadakis

doi: 10.12681/ta.36874

To cite this article:

Diamantopoulos, S., & Fragiadakis, M. (2024). Risk Assessment of Ancient Colonnades. *Technical Annals*, *1*(6). https://doi.org/10.12681/ta.36874

Risk Assessment of Ancient Colonnades

Spyridon Diamantopoulos[1][0000-0002-5104-4850] and Michalis Fragiadakis[1][0000-0002-0698-822X]

[1]National Technical University of Athens 9, Iroon Polytechniou st., 15780 Athens, Greece
sdiamadop@central.ntua.gr

Abstract. The paper introduces an innovative method to evaluate the fragility of ancient freestanding colonnades. It compares the seismic response and stability of colonnades with freestanding columns using a simplified modeling approach suitable for seismic design software. The methodology bypasses the need for time-consuming or complex simulations. Detailed discussion is provided on the performance criteria and the methodology for the fragility estimations. The case studies aim to address the proposed modeling and its effectiveness in simulating ancient structures and promptly generating accurate fragility curves. The Engineering Demand Parameter consistently focuses on column rotation over the slenderness angle, while various Intensity Measures are explored.

Keywords: ancient monuments, rocking structures, fragility, colonnades.

1 Introduction

In many cases, ancient structures consist of freestanding columns that are either monolithic or multi-drum. If the structure consists of more than one column that are capped by an architrave, then they form a colonnade. Such structures have survived powerful earthquakes over their lifetime and are of main interest for civil engineers. They can be found in archaeological sites and are commonly made of marble. This study primarily focuses on monolithic column configuration with emphasis on column arrays.

Ancient freestanding colonnades exhibit rocking behavior, and their behavior has similarities with the behavior of a monolithic rocking column, as discussed by Diamantopoulos and Fragiadakis [1]. The rocking column stands as a fundamental problem in earthquake engineering, initially addressed by Housner [2] who proposed its equation of motion. Many researchers, e.g. DeJong and Dimitrakopoulos [3] and Dimitrakopoulos and Giouvanidis [4], among others, have worked on this topic while Cheng [5], Palermo et al. [6] and Priestley and Tao [7] demonstrated the impressive lateral load stability of these structures. Moreover, Psycharis et al. [8] proposed a seismic fragility framework for ancient columns, introducing a fully Performance-Based Earthquake Engineering (PBEE) approach. This work highlights the characteristics of ancient multi-drum columns stacked rigidly atop one another using the Discrete Element Modeling (DEM).

The current study proposes robust modeling techniques for assessing the seismic response of monolithic rocking structures, e.g. rocking frames (Fig. 1). Moreover, it

presents a performance-based and rapid risk assessment framework for investigating their seismic response. The paper is built on previous research works of Diamantopoulos and Fragiadakis [1, 9], where it was demonstrated the Finite Element Modeling with simple beam elements and rotational springs with negative stiffness. This approach is easily extended to monuments yielding accurate solutions for a broad array of structures with members that can rock.

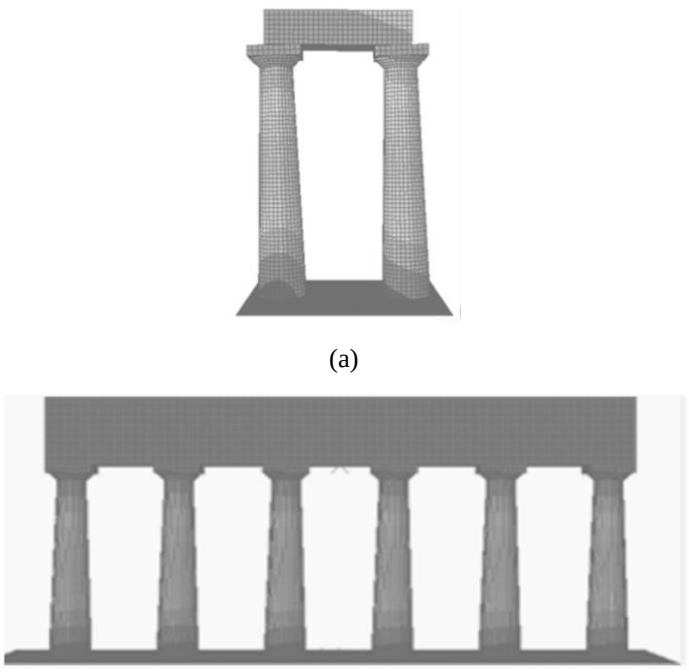

(a)

(b)

Fig. 1. Modeling of: (a) a rocking frame and (b) an array of freestanding columns using the Finite Element Method.

2 Simplified models for rocking colonnades

Colonnades that exhibit uplift and rocking behavior can generally be represented using the model of Figure 2. This model builds upon the single-column framework addressed in Diamantopoulos and Fragiadakis [9]. It involves nonlinear rotational springs located at the rocking interfaces, namely between the ground and the columns, as well as between the epistyle and the top of the columns. Parameters to be defined include the mass matrix and the restoring moment, M_{res}, of the system through the $M - \theta$ relationship of the rotational springs. Essentially, the proposed model addresses the generalized equation of motion governing a planar rocking structure, as initially studied in Diamantopoulos and Fragiadakis [1].

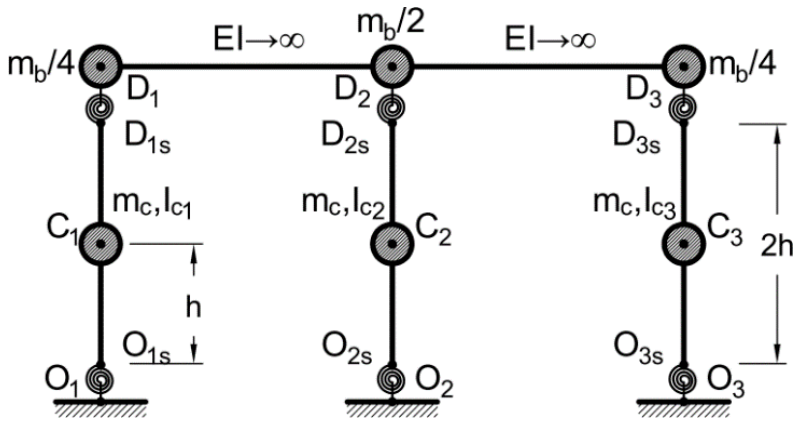

Fig. 2. A two-bay planar rocking structure using the proposed simplified modelling approach.

Based on Fig. 2, the mass of the piers is m_c, concentrated at their center of gravity and the mass of the deck/architrave is m_b, lumped at the nodes D_1, D_2 and D_3. Nonlinear springs are placed at the top and the bottom of the columns defining the total restoring moment. It is pointed out that sliding between the columns and the base or between the columns and the deck is always neglected. Furthermore, considering that the deck's mass is lumped at the top pivot point and its distance from the pivot point of the base is $2R$, it is assumed that the rotational moment of inertia at the center of gravity of each column is $I_{C1} = I_{C2} = I_{C3} = 1/3m_cR^2 + m_cb^2$. In the case of N columns, the epistyle mass is $m_b/(N-1)$ and $0.5m_b/(N-1)$ at the internal and the end nodes, respectively. The rotational moment of inertia at nodes D_{1s} and D_{Ns} will be equal to $I_{D1s} = ... = I_{DNs} = [0.5m_b/(N-1)](2b)^2$ and at nodes D_{2s}, . . . , $D_{(N-1)s}$ it will be $I_{D2s} = ... = I_{D(N-1)s} = 2I_{D1s}$. The M-θ relationship of each spring is obtained from the restoring moment and is different at the bottom and the top spring due to the different axial load:

$$M^{btm}(\theta) = m_c gR\sin\left(\alpha\,\mathrm{sgn}\,\theta - \theta\right) + \frac{m_b}{k(N-1)}gR\sin\left(\alpha\,\mathrm{sgn}\,\theta - \theta\right)$$

$$M^{top}(\theta) = \frac{m_b}{k(N-1)}gR\sin\left(\alpha\,\mathrm{sgn}\,\theta - \theta\right) \quad (1)$$

where $k = 1, 2$ for the internal and the two external columns, respectively. It is mentioned that $\gamma = m_b/(Nm_c)$ while the maximum restoring moment is obtained for $\theta = 0$. The proposed model is adopted for the fragility and risk estimations described in the next sections.

3 Fragility assessment framework

Fragility curves serve as an essential tool for assessing the seismic risk of a system. They were initially developed to separate structural analyses from the hazard analyses that are referred to by engineering seismologists. Fragility curves refer to the probabilities of exceeding a damage state and thus these probabilities should be calculated. This probability is calculated conditioned on the seismic intensity and is referred to an Engineering Demand Parameter (*EDP*) that exceed a specified threshold *edp*:

$$F_R\left(IM\right) = P\left(EDP > edp \mid IM\right) \tag{2}$$

To calculate Eq. 2 three possible response cases are considered: (i) system at rest, (ii) system uplifted and (iii) system overturned. With the aid of the total probability theorem, the fragility can be calculated following the equation:

$$F_R = P\left(EDP \mid NoUplift\right) P_{NoUplift} + P\left(EDP \mid Uplift\right) P_{Uplift} + P\left(EDP \mid Ovtn\right) P_{Ovtn} \tag{3}$$

where *P(EDP | NoUplift)*, *P(EDP | Uplift)* and *P(EDP | Ovtn)* are the damage-state exceedance probabilities for *no-uplift*, *uplift* and *overturning*, respectively. For columns that will not uplift or overturn, *P(EDP | NoUplift)* = 0 and *P(EDP | Ovtn)* = 1, respectively. Thus, the fragility curve calculation is simplified to:

$$F_R = P(\,EDP \geq edp \mid Uplift\,)(1 - P_{Ovtn} - P_{NoUplift}\,) + P_{Ovtn} \tag{4}$$

It should be mentioned that rocking data are assumed as lognormally distributed. Hence, *P(EDP ≥ edp | Uplift)* is calculated once the mean and the standard deviation of the logs of the *EDP*, denoted as μ_{logEDP} and σ_{logEDP} [11], respectively, are known. Once they are known they can be used to calculate the probability that the *EDP* exceeds a threshold *edp*:

$$P(\,EDP \geq edp \mid Uplft\,) = 1 - \Phi\left(\frac{log(\,EDP\,) - \mu_{logEDP}}{\sigma_{lnEDP}}\right) \tag{5}$$

where Φ is the standard normal distribution. The risk can be expressed as the mean annual frequency (MAF) of exceeding a damage-state. Adopting the PEER's formula, the damage-state MAF is:

$$\lambda_{EDP} = \int_{IM} P(\,EDP \mid IM\,)\left|\frac{d\lambda_{IM}}{dIM}\right| dIM \tag{6}$$

where $d\lambda_{IM}$ is the slope of the hazard curve. The MAF is obtained convolving the slope of the site hazard curve λ_{IM} with the fragility curve P(EDP|IM) that is defined with respect to the EDP and the IM considered. The hazard curve is assumed known from site hazard analysis studies, as discussed in reference [13].

4 Fragility analysis methods

4.1 Multiple stripe analysis

Multiple stripe analysis provides a nuanced understanding of how the system's vulnerability changes as seismic intensity increases, allowing for more targeted risk assessment strategies. In the case of rocking structures, the damage-state fragility curves can be calculated using severe approaches or methods. The Incremental Dynamic Analysis (IDA) proposed in Ref. [10] is a valuable tool for such problems. In the IDA method, the system examined is subjected to ground motion records scaled to multiple intensity levels. Single record capacity curves are then produced as has been discussed in Diamantopoulos and Fragiadakis [12] and Fragiadakis and Diamantopoulos [13].

Multiple Stripe Analysis (MSA) method is another approach that has similarities to the IDA. In this case, the records are scaled to the same IM and thus the EDP values form a stripe. Stripes allow the direct calculation of the 50%, the 16% and 84% percentile capacity curves conditional on the IM. It should be mentioned here that in IDA the scaling factors are different, but the data can be converted to a stripe form using the interpolation method. In this work only MSA was performed.

If the *EDP* values form stripes conditional on the *IM* value, Eq. 4 is solved using an approach based on multiple stripe analysis. For every stripe, the mean and standard deviation conditional on the *IM*, are easily calculated. Considering the assumption that the data follow the lognormal distribution, the fragility is obtained as:

$$F_R = \Phi\left(\frac{\mu_{logEDP} - log(edp)}{\sigma_{logEDP}}\right)\left(1 - P_{Ovtn} - P_{NoUplift}\right) + P_{Ovtn} \tag{7}$$

$P_{NoUplift}$ and P_{Ovtn} are determined as the proportion of simulations where there was no uplift and overturning, respectively. This is obtained for every stripe, i.e. $P_{NoUplift}$ and P_{Ovtn} are calculated as the number of simulations of *NoUplift* or *Ovtn* over the total number of simulations, respectively.

4.2 Cloud analysis method

In case of unscaled, or scaled with the same factor, ground motions, they are not stripped and thus the data form a cloud. Thus, cloud analysis should be adopted to calculate the fragility curves. The mean value of the logarithms (μ_{logEDP}) and a single constant value for the dispersion σ_{logEDP} are provided through a linear fit. Knowing μ_{logEDP} and σ_{logEDP} and using Eq. 7 it is possible to calculate the fragility of the rocking simulations. The latter requires knowledge of P_{NoRock} and P_{Ovtn}. These probabilities can be obtained with a logistic regression model which yields a probability estimation as a function of the *IM*. Therefore, for the *NoUplift* and *Ovtn* cases the probabilities are:

$$P_{NoUplift} = \frac{1}{1+e^{-(b_1+b_2 log(IM))}}$$
$$P_{Ovtn} = \frac{1}{1+e^{-(b_3+b_4 log(IM))}} \quad (8)$$

where the constants b_1, b_2, b_3, b_4 are the parameters of the logistic regression model, obtained with binomial-based, generalized linear model (GLM) regression.

4.3 Maximum-Likelihood (MLE) fitting

The maximum-likelihood (MLE) fitting [14] is adopted in both striped and cloud data. The MLE fitting approach fits the Cumulative Distribution Function (CDF) of a lognormal distribution on the EDP-IM plane. The fragility function is simply a lognormal CDF of the form:

$$F_R = P(EDP \geq edp) = \Phi\left(\frac{log(EDP/\theta_a)}{\beta_a}\right) \quad (9)$$

where θ_a and β_a are determined by maximizing the likelihood function and are the median and the dispersion.

In fact, Multiple-stripe analysis provides the number of successes n_{suc}, i.e. the number of simulations that the damage-state has been exceeded after n_{tot} total simulations. Using the binomial distribution on the data of a single stripe, the probability of n_{suc} successes after n_{tot} simulations, is defined as:

$$P(Success = n_{suc}) = \binom{n_{tot}}{n_{suc}} P(EDP^{(s)})^{n_{suc}} (1 - P(EDP^{(s)}))^{n_{tot}-n_{suc}} \quad (10)$$

If there are k stripes, the MLE function is obtained substituting Eq. 9 to Eq. 10 as follows:

$$L = \prod_{i=1}^{k} \binom{n_{tot,i}}{n_{suc,i}} \Phi\left(\frac{log(EDP/\theta_a)}{\beta_a}\right)^{n_{suc\,j}} \left(1 - \Phi\frac{log(EDP/\theta_a)}{\beta_a}\right)^{n_{tot\,j}-n_{suc\,j}} \quad (11)$$

The only variables to be determined are θ_a and β_a, which are identified as the values that optimize the likelihood function of Eq. 11. It's important to highlight that the fitting process encompasses the entire dataset, a task readily accomplished with a basic computer script. In cases where the EDP-IM pairs form a cloud, each simulation is considered a distinct stripe. Consequently, k represents the number of simulations, while n_{tot} is set to one ($n_{tot} = 1$), and n_{suc} equals one or zero, depending on whether the simulation surpasses the damage-state threshold or not, respectively.

5 Numerical results and discussion

The structure under examination is a colonnade consisting of N = 3 columns of equal height. The colonnade possesses the following properties: 2h = 5m, 2b = 0.75m, and $\gamma = m_b/(3m_c) = 1$, where m_b represents the mass of the epistyle, and m_c signifies the mass of each column. Moreover, the colonnade is topped with a rigid beam weighing the sum of the weights of the columns. To validate the proposed modeling approach, the structure is subjected to both near-field and far-field ground motions. As illustrated in Fig. 3, the results obtained using the proposed model depicted in Fig. 2 are compared against the equation of motion governing the problem. Remarkably, for both seismic records, a high degree of agreement is observed, confirming the precision of the proposed model.

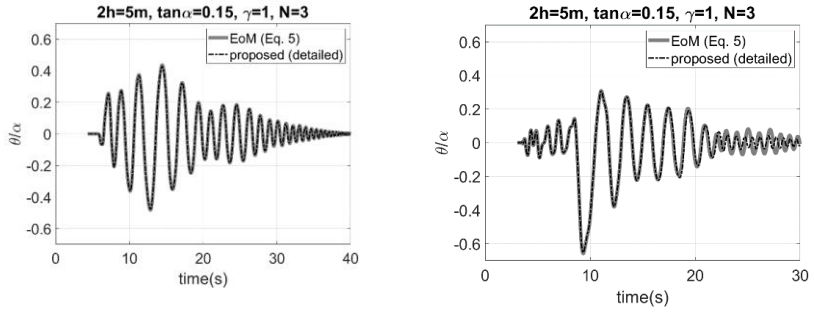

(a) (b)

Fig. 3. Evaluation of the colonnade's response using the suggested model under: (a) a Loma Prietta 1989, Saratoga - Aloha Ave, PGA=0.36g (near-field), (b) Northridge 1994, MUL279 component, PGA=0.52g (far-field).

Fragility analysis was conducted using a set of thirty ground motions representing a scenario earthquake. Three damage-states corresponding to θ/α= 0.15, 0.35, and 1.00 were considered, with the chosen intensity measure (IM) being the normalized peak ground acceleration, *PGA/gtanα.* In Fig. 4a fragility curves derived with different approaches are compared. Smooth curves represent Maximum Likelihood Estimation (MLE) fitting, while non-smooth curves were generated using Eq. 9. Notably, the two approaches exhibit close results.

Fig. 4b compares fragility curves derived from cloud analysis with those from multiple stripe analysis. While the fragility curves coincide for the two damage-states, differences are observed for the overturning damage-state. Insufficient records at high IM values bias fragility curves in cloud analysis. Furthermore, Fig. 5 compares the response of the colonnade with a single column using PGA/gtanα and PGV as IMs. All fragilities were determined using the MLE approach on stripped data. Overall, it is mentioned that colonnades demonstrate greater stability compared to single columns irrespective of the IM. However, IM selection does not impact the fragilities of the two lower damage states, but it does for the near-collapse damage-state.

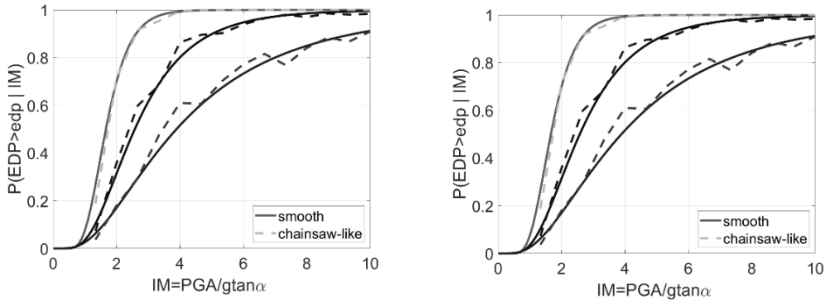

(a) (b)

Fig. 4. (a) Definition of smooth fragility curves, (b) comparison of multiple stripe and cloud analysis. The damage-states considered are θ/α = 0.15, 0.35 and 1.00.

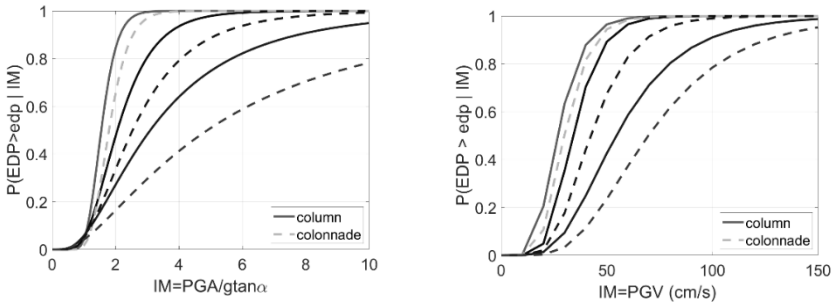

(a) (b)

Fig. 5. Comparison of a column with a colonnade in case of N=3 (γ=1, 2h=5.0m, 2b=0.75m) using the fragility functions: (a) IM=PGA/gtanα, (b) IM=PGV. The damage-states considered are θ/α = 0.15, 0.35 and 1.00.

6 Conclusions

The paper presents a Performance-Based Earthquake Engineering (PBEE) framework for the fragility assessment of ancient structures mainly suitable for monolithic freestanding columns or colonnades. The numerical investigation validates the effectiveness of the modeling approach in addressing various scenarios and providing precise estimations. Initially, the simple models, relying on the direct stiffness method, offer a robust way to analyze different colonnade configurations that use basic structural assessment tools. Their advantage lies in reducing the computational cost by avoiding complex relationships for the body interactions and the energy loss assessment. The latter are often required in commercial Finite Element Method (FEM) or Discrete Element Method (DEM) models. Furthermore, it is mentioned that the Engineering Demand Parameter (EDP) is consistently the normalized rotation θ/α, while

different options for the Intensity Measure (IM) are considered. The fragility assessment is performed using either a cloud or multiple stripe analysis approach. Special attention is warranted for simulations that overturn or do not uplift the structure.

References

1. Diamantopoulos S, Fragiadakis M. Modeling of rocking frames under seismic loading. Earthquake Engineering & Structural Dynamics 2022; 51 (1): 108–128.
2. Housner G. The behavior of inverted pendulum structures during earthquakes. Bulletin of the Seismological Society of America 1963; 53(2): 404–417.
3. DeJong M, Dimitrakopoulos E. Dynamically equivalent rocking structures. Earthquake Engineering and Structural Dynamics 2014; 43(10): 1543–1563.
4. Dimitrakopoulos E, Giouvanidis A. Seismic response analysis of the planar rocking frame. Journal of Engineering Mechanics 2015, 141(7):04015003.
5. Cheng C. Shaking table tests of a self-centering designed bridge substructure. Eng Struct 2008; 30(12): 3426–3433.
6. Palermo A, Pampanin S, Marriott D, Design, modeling, and experimental response of seismic resistant bridge piers with posttensioned dissipating connections. J Struct Eng 2007; 133(11): 1648–1661.
7. Priestley M, Tao J. Seismic response of precast prestressed concrete frames with partially debonded tendons. PCI J 1993; 38(1):58–69.
8. Psycharis IN, Fragiadakis M, Stefanou I (2013). Seismic reliability assessment of classical columns subjected to near-fault ground motions. Earthquake Engineering & Structural Dynamics 2013; 42:2061-2079.
9. Diamantopoulos S, Fragiadakis M. Seismic response assessment of rocking systems using single degree of freedom oscillators. Earthquake Engineering & Structural Dynamics 2019; 48(7), 689–708.
10. Vamvatsikos D, Cornell CA. Incremental dynamic analysis. Earthq Eng Struct Dyn. 2002; 31(3):491–514.
11. Vamvatsikos D, Fragiadakis M. Incremental Dynamic Analysis for seismic performance uncertainty estimation. Earthq Eng Struct Dyn. 2009; 39(2): 119-235.
12. Diamantopoulos S, Fragiadakis M, Modeling, fragility and risk assessment of ancient freestanding columns and colonnades, Engineering Structures 2023, Volume 275, Part B, 115273.
13. Fragiadakis M, Diamantopoulos S. Fragility and risk assessment of freestanding building contents. Earthquake Engineering & Structural Dynamics 2020; 49 (10): 1028-1048.
14. Baker JW. Efficient analytical fragility function fitting using dynamic structural analysis. Earthquake Spectra 2015; 31(1):579–599.